Contribution of material and manufacturing process in fatigue design

Pascal Daguier*, Jean-Michel Jachmich, Gilles Baudry

ASCOMETAL CREAS, Avenue de France,
BP70045, 57301 Hagondange cedex
* p.daguier@ascometal.lucchini.com

Abstract To fulfil pollution standards, new motorizations of cars and trucks needs more efficient, more reliable, and naturally cheaper components. Consequently, steel must be more efficient, just-fitted to the application, and must contribute to global component cost reduction. This paper illustrate by few examples some evolution of steel (grades, cleanliness and associated heat treatments or surface treatments) performed to face these evolutions in the case of the most critical component of a car or of a truck. It presents also a comparison of steel with alternative materials in terms of durability.

1 INTRODUCTION

The Kyoto agreement on climate change led many countries to agree to reduce their CO_2 emissions over the next few years. One of the major sources of CO_2 comes from the use of cars and trucks, and it's anticipated that major reductions of CO_2 could be achieved by the development of fuel efficient vehicles (indeed, fuel consumption and CO_2 emission of a vehicle are two indissociale parameters). In Europe, significant improvements in fuel economy should be done in the next few years, since the European Union fixed that the average CO_2 emission level should be 140g/km or less by cars, which represents a reduction by 25% compare to the reference level of 1995. For 2012, the objective is at 120g/km, which correspond to a fuel saving of nearly 30%.

Two reach this goal, 2 ways are examined by carmakers:

- Lightening of vehicles
- Increase the efficiency of engine

Downsizing of component or increase the efficiency of engine lead to higher stresses in the overall of mechanical parts (conrods, crankshaft, gears…). To face such increase of mechanical loading, steel maker has to develop new steel grades, adapted to each application. For that, a clear understanding of the way the components are made, used and fail is a key parameter for developing adapted metallurgies

In this article, we will show two examples of development of new methodologies and steel grades to face such increase of fatigue properties, in both side of downsizing (like for helical suspension springs) or increasing of applied loading for the same geometry (like for gear steel).

At the end, we will discuss about the design of components for very high cycle fatigue domain and the consequence on materials.

2 HELICAL SUSPENSION SPRINGS

The suspension systems of cars, which represent around 12-15% of the weight of the car, are concerned by downsizing [**1**]. Considering the helical spring as an important part of the suspension system, the weight reduction is obtained by a decrease of the bar diameter and the number of spring coils. These evolution leads to a decrease of the average weight of a helical spring from 4 kg in 1975 to 2kg nowadays. In this respect, the stress level applied on the spring is increased, and the steel used to manufacture these springs needs to have high mechanical properties to achieve a good fatigue resistance and also a good sag resistance.

The corrosion resistance is also important for this application. Indeed, during service, the protective coating applied on the springs can be scratched by gravels, and bare underlying metal can be put in contact with the atmosphere, including humidity, drops of rain but also de-icing salts. Generally speaking, an increase of mechanical properties decreases the corrosion fatigue resistance of the steels. In this respect, a compromise needs to be found, that is why the study of corrosion fatigue resistance is very important.

Cars and spring makers develop their own test to evaluate the influence of corrosion on fatigue strength of helical suspension spring steel, ranging from totally dissociated conditions to coupled fatigue corrosion. So the development of a new steel grades should fulfil these two requirements.

For that, an original device and test procedure have been set up to test in torsion spring steels with 3 types of conditions :

- Fatigue in air (taken as the reference level)
- dissociated corrosion fatigue (specimens is pre-corroded in a climatic chamber and then tested in fatigue in air)
- coupled corrosion fatigue (specimens placed in a corrosion cell fixed on a hydraulic fatigue testing machine – corrosion and fatigue loading are applied at the same time)

The target being high strength springs (to face the decreasing of diameter of the spring), two spring steel grades, 60SCV7+Nb and 45SCV6, allowing achieving a very high tensile strength of 2100 MPa have been selected (see table 1). The specimens are shot-peened and painted (The thickness of the painting is around 200 µm) in the same conditions as commercial springs. The painting is locally removed using laser heating, consisting in a local vaporisation of the painting, giving rise to bare metal areas without any mechanical indentation of the metal to simulated damage induced by gravel.

table 1: mechanical characteristics of steel grades

grade	YS (MPa)	UTS (MPa)	Elongation (%)	reduction of area (%)
60SCV7+Nb	1886	2139	9	32
45SCV6	1774	2062	9	41

For fatigue in air, S-N curves have been plotted for the 2 steel grades, the conditions chosen were the following: a mean stress fixed for all the tests and equal to 856 MPa (which correspond to the weight of the vehicle), and alternate stresses .For dissociated and coupled corrosion fatigue, results will be presented for only one maximal stress of 1350 MPa.

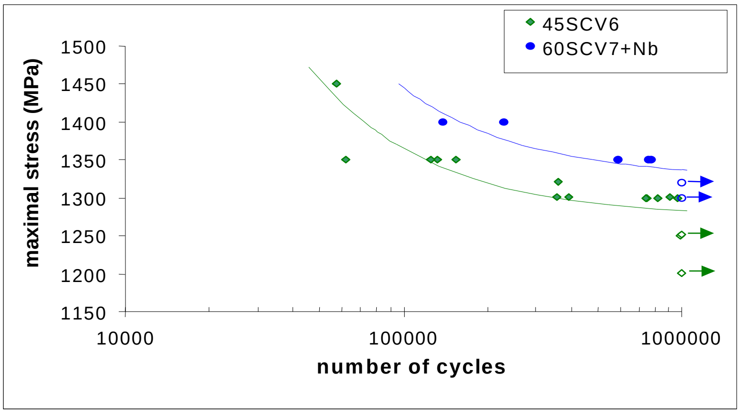

Figure 1 : S-N curves obtained in air for the 2 grades 60SCV7+Nb and 45SCV6; maximal stresses are plotted, for a constant mean stress of 856 MPa; open marks with arrows mean not fractured; tests were stopped at 10^6 cycles if specimens were not fractured

Fatigue limits have been evaluated using the adjustment $N = A / (\tau - \tau_D)$ and are reported in table 2. The fatigue limit is directly in relation with UTS.

table 2 : fatigue limit at 10^6 cycles estimated and expressed in maximal stress (for mean stress = 856 MPa); relative fatigue limit regarding the UTS is also reported

grade	fatigue limit τ_D (MPa)	ratio τ_D/UTS
60SCV7+Nb	1325	0,62
45SCV6	1274	0,62

The results of dissociated corrosion fatigue are shown in Figure 2.

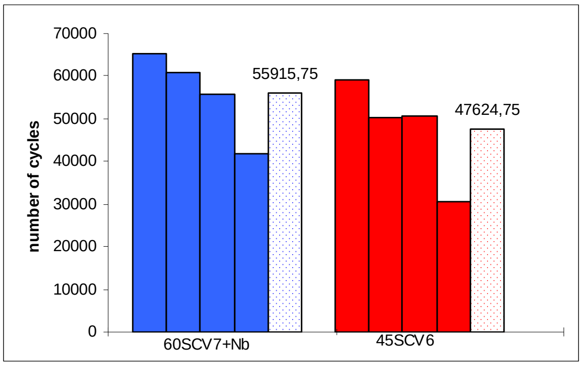

Figure 2: comparison of the dissociated corrosion fatigue life for the 2 grades 60SCV7+Nb, and 45SCV6; the stress applied is $\tau = 856 \pm 494$ MPa; 4 specimens have been tested for each grade (coloured bars); the average value is also reported (right bar for each grade)

We can notice that there are no significant differences between the 2 grades. We will discuss this result below considering the mechanisms. When we compare the dissociated corrosion fatigue life with the fatigue life in air, we notice that the life sharply decreases. Comparing the results of Figure 1 with those of Figure 2 at 1350 MPa, we see that the ratio of corrosion fatigue to fatigue in air is around 10% for grade 60SCV7+Nb and 15% for grade 45SCV6. Thus, a corrosion stage prior fatigue testing decreases significantly the life compared to tests in air.

When testing the specimens previously corroded by fatigue in air, the crack always initiates on a corroded area, clearly visible on Figure 3 as a dark area. On the fracture surface, this corroded area corresponds to a corrosion pit which acts as a crack initiation site. This corrosion pit gives rise to a local stress concentration, which induces a crack at its bottom (). This type of fracture is observed for the 2 steel grades.

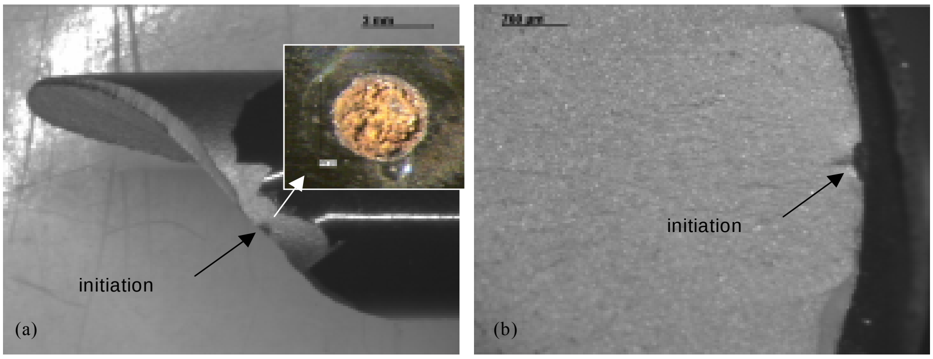

Figure 3: fracture produced by dissociated corrosion fatigue on a specimen of grade 45SCV6; (a) lateral surface with zoom view of the corrosion products; (b) fracture surface

The corrosion pits being formed prior the fatigue testing, we assumed that they act as a initial defect. In this respect, a fatigue limit should exist for dissociated corrosion fatigue tests. We used the theory of Murakami, who determined the fatigue limit in torsion for specimens with initial surface defects [**2**]. According to this theory, the fatigue limit τ_w for 10^7 cycles in alternate torsion (R= τ_{min} / τ_{max} = - 1) can be estimated according to:

$$\tau_w = \frac{0.93}{F(b/a)}(HV + 120).\frac{1}{\sqrt{area_p}^{1/6}}$$

with HV the Vickers hardness, $area_p$ the area of the defect on the surface of fracture, $F(b/a)$ a 4th degree polynomial function given by :
$F(b/a) = 0.0957 + 2.11(b/a) - 2.26(b/a)^2 + 1.09(b/a)^3 - 0.196(b/a)^4$

The results obtained are extrapolated to the experimental R ratio with a Goodman-smith diagram. The fatigue limit are reported in table 3

table 3: calculated fatigue limits at 10^6 cycles corresponding to dissociated corrosion fatigue, compared to experimental fatigue limit in air ; the ratio between the 2 is also reported

grade	calculated fatigue limit for dissociated fatigue corrosion (MPa)	experimental fatigue limit in air (MPa)	ratio fatigue limit in corrosion / fatigue limit in air
60SCV7+Nb	1061	1325	0.80
45SCV6	1068	1274	0.84

We notice that limit for dissociated corrosion fatigue is at least 200 MPa less than fatigue limit in air. Nevertheless, the ratio between fatigue limit in corrosion and fatigue limit in air remains high, around 0.80. It means that mechanical effects remain very important.

Figure 4 show fatigue lifetime obtained in coupled corrosion on 4 or 5 specimens tested at mean stress = 856 MPa and maximal stress = 1350 MPa .

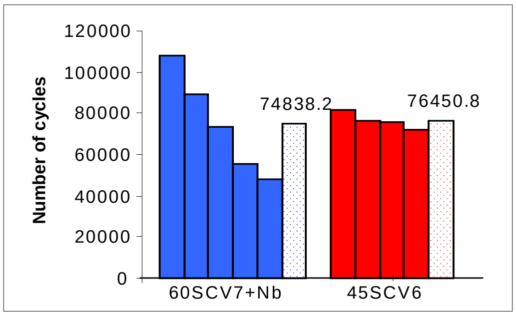

Figure 4: comparison of the coupled corrosion fatigue life for the 2 grades; the stress applied is $\tau = 856 \pm 494$ MPa; 4 or 5 specimens have been tested for each grade (coloured bars); the average value is also reported (right bar for each grade)

As for dissociated corrosion fatigue, there is no significant difference from one grade to the other. All the specimens present a crack initiation on the corroded areas. The life duration is again decreased compared to fatigue in air, and the ratio between life in coupled corrosion fatigue and fatigue in air lies between 15% and 17% for the 2 grades.

If fatigue life obtained in dissociated corrosion fatigue and coupled fatigue seems to be equivalent, we should consider that the total corrosion time is very different in the two tests. For dissociated corrosion fatigue test, the duration of the cyclic corrosion test is 4 weeks, with a total salt spray time of 96 hours. For coupled corrosion fatigue, the total time of salt spray is only 1 h. It is almost 100 times less, however the ratio of number of fatigue cycles is not in a ratio of 100. So it shows that there is a synergistic effect between corrosion and fatigue for coupled corrosion fatigue, which contributes to a more severe mechanism. Indeed, fractographic examination show that

- corrosion pits are smaller and less visible at small magnification compared to dissociated corrosion fatigue

- crack propagation is assisted by hydrogen diffusion into the metal. Indeed, some intergranular fracture is observed on the fracture surface of grades 45SCV6 and 60SCV7+Nb (Figure 5), which could be attributed to hydrogen embrittlement [**3**].

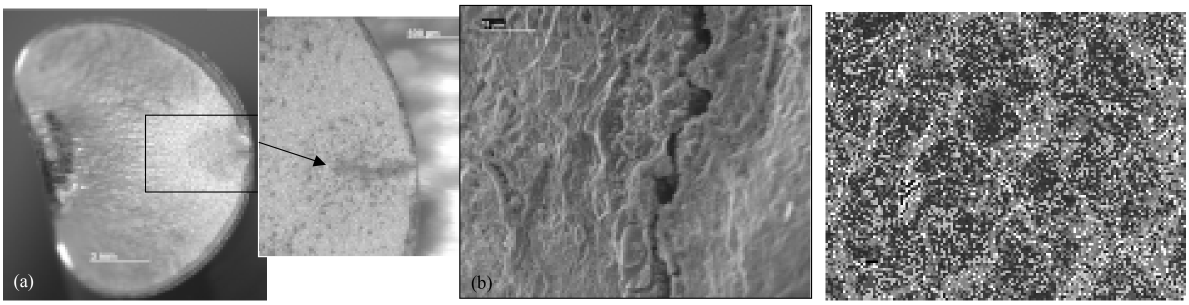

Figure 5: (a) small magnification optical view of the fracture surface of a specimen of 45SCV6 ; (b) SEM observation of a crack containing corrosion products; (c) detail of the fracture surface of a specimen of grade 60SCV7+Nb

Further test performed on 60SCV7 in air and coupled fatigue corrosion but on unpeened specimens are plotted in Figure 6. In this case, and contrary to dissociated fatigue corrosion, no asymptotic regime in obtained. For long fatigue test (low stress level), corrosion has more impact on fatigue strength compare to test performed at high stress level, for which no difference has been found between dissociated and coupled fatigue corrosion.

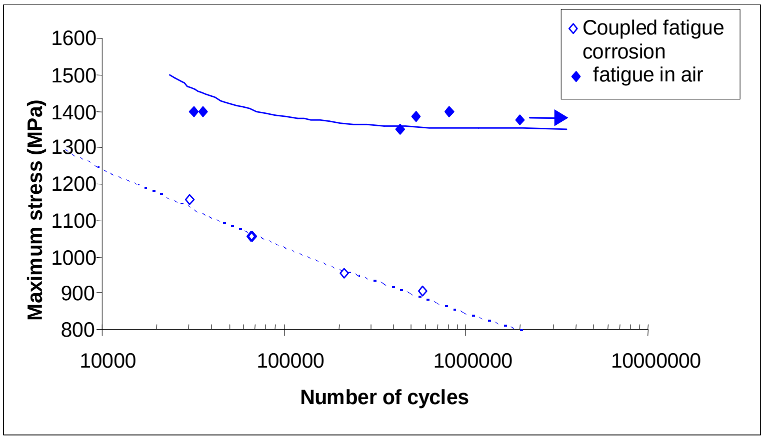

Figure 6 : comparison of S-N curves of 60SCV7 obtained by fatigue in air and in coupled fatigue corrosion

3 STEELS FOR GEARBOXES APPLICATIONS

In the case of gearboxes, car makers are face, from several years, to an increase of the torque of this component. In 10 years, the torque was twice more important than those anticipated during the design of the gearbox (Figure 7). In parallel, the weights of gearboxes increase very slowly.

Research for new gear steel for high loading application need a precise understanding of the different mechanisms which are responsible of fatigue and/or mechanical failure. For the steel maker, it's important to develop fatigue test reproducing damage during in-service conditions of the real component on simpler geometries to test various steel analysis and/or case-hardening treatment

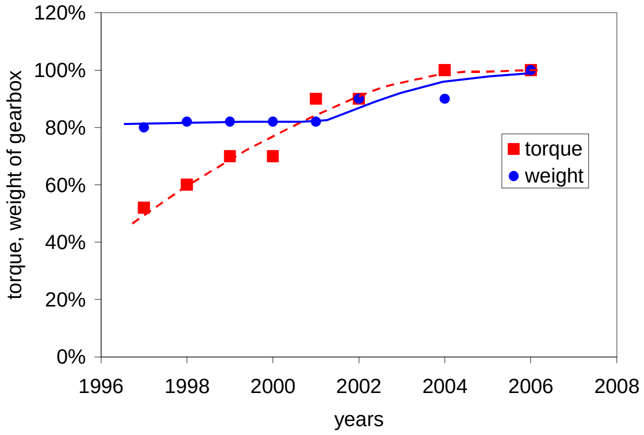

Figure 7 Example of evolution of torque and weight of gearbox

Figure 8 presents the position of maximum stresses in the contact between gear teeth. Two main kind of damage could appear during the in service conditions:

- Bending fatigue at the root tooth
- Rolling contact fatigue (pitting, micropitting) and/or wear / scuffing in the flank of the gears, depending of the contacting surface roughness and oil viscosity.

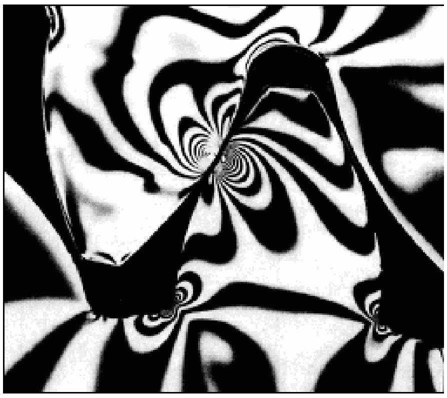

Figure 8 localisation of maximum stresses during contact between gear teeth

A third type of failure is now more and more taken into account by car-makers in the design of gears and the choice of the case hardening treatment : it's mechanical failure due to over stresses or impacts on gear teeth.

The optimisation of either bending fatigue strength, rolling contact strength and impact resistance need to find a compromise. Indeed, to face the increase of loading on gear teeth, the case depth could be increased to improve bending and rolling contact fatigue strength. But this way dramatically imparts impact resistance. Tricot and al. [**10**] have shown the influence of case depth on the bending strength during impact. 3 regimes could be identified with case depth, it's mean a plateau regime for low and high case depth and a transition for intermediate one (Figure 9).

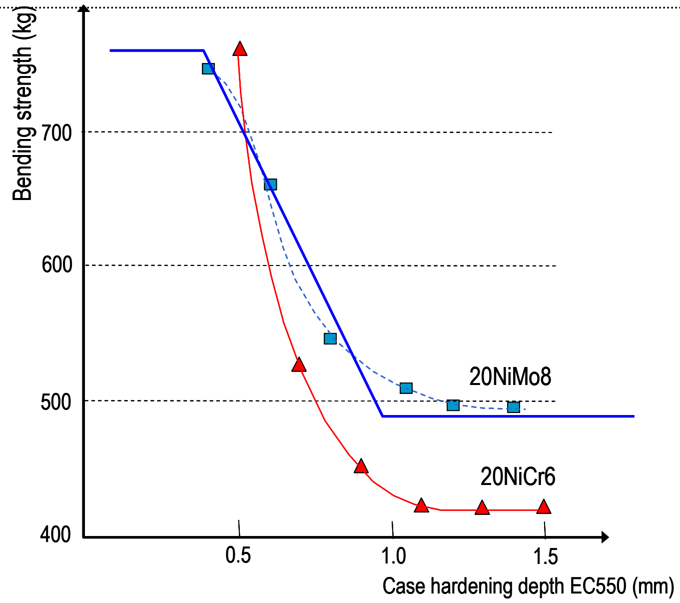

Figure 9 influence of case depth on bending strength (see [10])

A fit performed in the transition regime show that the evolution vary with $1/\sqrt{P_C}$, where Pc is the case depth. Then, the case depth could be seen as equivalent to a critical defect for the fracture of the piece.

So, a fracture mechanic type model has been developing to modelize the influence of component geometry, size and case depth on the fracture energy. This approach allows us to know the respective contribution to the geometry and the material on the impact energy and separate them. The results have been compared to data published by [**11**] and are presented in Figure 10. If the order of magnitude are found by this simple modelization, these first results highlights the need for data concerning the influence of carburizing & quenching conditions on mechanical properties of case and core.

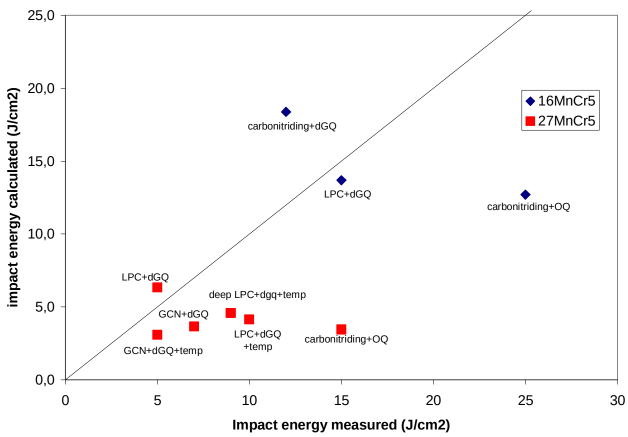

Figure 10 : Modelization of impact strength of case hardened steel / comparison with experimental data

To go further in the understanding of the relation between thermo-chemical treatment and the mechanical properties (bending fatigue / impact toughness), several case have been studied and are summarised in table 4. Rotative bending test have been performed to simulate the bending of gear teeth and impact test on Charpy type specimen have been used to evaluate the impact strength. Metallurgical characterisation performed on each treatment are summarised in table 4.

table 4 : Case hardening treatment and metallurgical characterization

case hardening treatment	hardness Hv0.5 -50µm from surface	Core hardness Hv0,5	EC650 [µm]	ASTM grain size (case)	ASTM grain size (core)	retained austenite -25 µm from surface	core	case
low pressure carburizing direct gaz quenching	796-842	508-520	480	8/9 few 6	8/9 few 6	25,1	M+B	RAS
low pressure carburizing direct gaz quenching+tempering	727-738	457-476	430	8/9 few 6	8/9 few 6	20,7-24,5	M+B	RAS
gaz carbonitriding + oil quenching	760-804	515-523		8/10 few 6	8/10 few 6	25.6 / 26.8	M+B	oxydation 15-20 µm
low pressure carburizing+step quenching	787	475	460	8/9	8/9	24,3	M+B	RAS
low pressure carbonitriding direct gaz quenching	789-805	528	450		9/11	20,5	M+B	RAS
low pressure carbonitriding+step quenching	763-790	525	470		8/11	26,1		RAS

The results of such experiments are summarised in Figure 11.

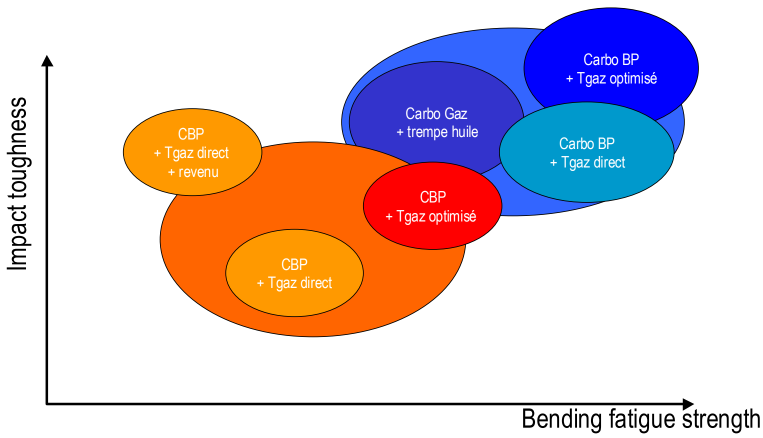

Figure 11: optimisation between bending fatigue strength and impact toughness

Theses results highlight the influence of carburizing treatment and quenching conditions on the optimisation between bending fatigue strength and impact strength, mainly the difference between carburizing and carbonitriding and the influence of hot oil and/or step quenching around 140-180°C. These results are in agreement with those published by Da Costa at al.[**11**]. However, steel grade is much more important than carburizing and quenching conditions on the compromise, mainly by its chemical analysis which determine the core hardness and the microstructure obtained after quenching both in the case and in the core. Those microstructures strongly influence fatigue and impact behaviour. Figure 12 summarised the influence of carburizing conditions on fracture mode obtained on impact specimen. The share between ductile and brittle mode of fracture have been determined by SEM. The analysis clearly shows that high impact energy is associated to ductile fracture mode in the case but also in the core.

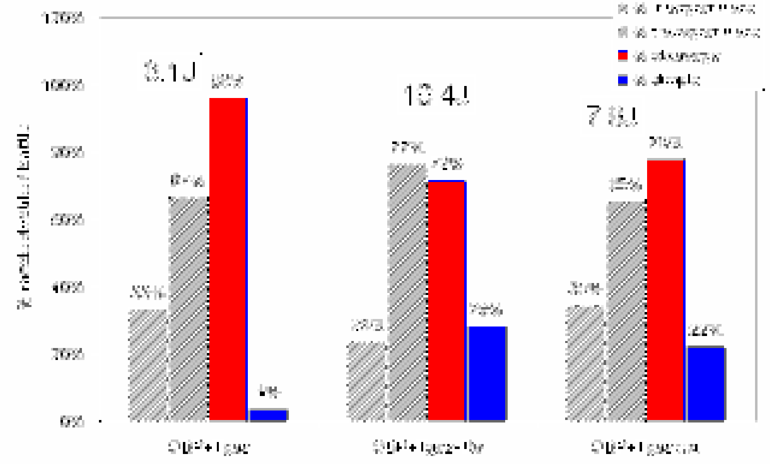

Figure 12 : influence of carburizing & quenching conditions on fracture mode of impact specimens

4 MATERIALS FOR DESGIN IN THE VERY HIGH CYCLE FATIGUE REGIME

The increase of reliability required by carmakers to guarantee a car duration of about 300.000 km, combined with the current downsizing trend, leads to reconsider security factor used in the design of various components. Indeed, a guarantee of 300.000 km is equivalent, for various components of the powertrain, to a number of cycles of 10^8 to 10^{10}. Thus, the knowledge of the fatigue behaviour in this lifetime domain is essential, because too high safety factors reduces the competitiveness of the component, but too low safety factors leads to in-service failure.

However, as the generation of experimental data in the very high cycle fatigue (gigacyclic) domain is very difficult with present test facilities, the current designs are based on experimental data obtained up to 10^7 cycles (megacyclic fatigue), and then extrapolated to 10^8-10^{10} cycles (gigacyclic fatigue). This implies the existence of an endurance limit at about 10^7 cycles deduced from the shape of the experimental data obtained up to 10^7 cycles (WOHLER or S-N curve) and the statistical processing of this curve. The aim of the study was to develop a new technique of laboratory able to generate fatigue data on main engineering steels and alternative materials up to 10^{10} cycles, to provide data for mechanical parts design.

Indeed, for a conventional fatigue machine working at 20Hz, it needs 6 years to test one sample, compare to 6 days with a high frequency testing machine working at 20 kHz.

So, a testing device has been developed by the CNAM [**8**]. It's composed by a high frequency sonic energy converter and an acoustic amplifying horn, which stresses the test-specimen on its self-resonant frequency (20 or 30 KHz).

Several materials (see table 5) have been tested in this study. Their mechanical characteristics correspond to a wide range of UTS (Ultimate Tensile Strength), and thus a great range of performance levels. They include the main cast, forged and drawn materials used for the main automobile parts (parts of power unit: injection pumps and injectors, con-rods, crankshafts, valve springs, cylinder heads, gears …), or of suspension parts : suspension arms, steering knuckle, suspension springs, bearings (including spindles)...).

table 5 : Steel grades & microstructures used in the study

Grade	microstructure	UTS	application
100Cr6	martensite	2500	rolling bearing
	bainite	2500	rolling bearing
42CrMo4	Q&T martensite	1510	
		1035	
XC70	pearlite	930	hub units
35MnV7	bainite	890	crankshaft
38MnSiV5	ferrite-pearlite	880	crankshaft
cast iron GS51		795	
cast aluminium AS5U3G		220	

A particular attention was put to high frequency tests (20 and 30 KHz), to make them reliable, and in particular to validate them by comparing the S-N curves obtained in gigacyclic domain and in classical megacyclic domain in their common fatigue life domain (10^6-10^7 cycles). All the results obtained in gigacyclic domain are in good agreement with those obtained by conventional methods in the fatigue life range common to both experimental techniques (10^6 - 10^7 cycles). In the case of 100Cr6, the S-N curve show that the materials can fail between 10^6 and 10^{10} cycles, and thus the concept of fatigue endurance limit does not apply in this case. Some materials present a quasi asymptotic S-N curve, whereas others materials present a continuously decreasing curve accompanied by a reduction of the fatigue resistance reaching values up to 25% between 10^7 and 10^{10} cycles. It's quite obvious that these fatigue endurance limit variations should be taken into account in the design of components submitted to high number of cycles. Figure 13, presents the relative decrease of fatigue limit between 10^7 and 10^{10} cycles (i.e. divided by the endurance limit at 10^7 cycles) $[(\sigma_D(10^7) - \sigma_D(10^{10}) / \sigma_D(10^7)]$.

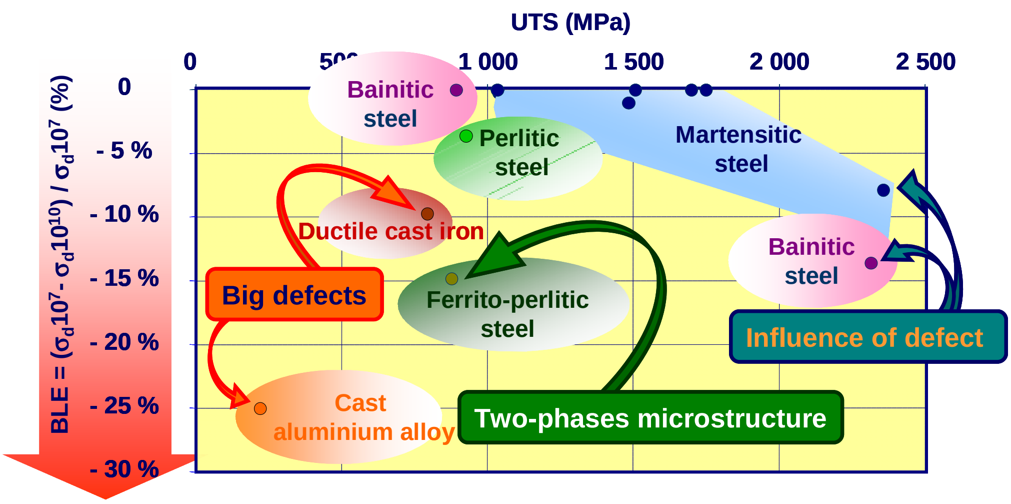

Figure 13 : Evolution of fatigue limit for different materials between 10^7 and 10^{10} cycles, R=-1

The analysis of these results shows that for martensitic steels, for which data are available in the UTS range (1 000 - 2 500 MPa), the decrease of fatigue limit between 107 and 1010 cycles increases with UTS, confirming the results obtained by other authors [**7**], or previously by ourselves with the same technique [**9**] or in rotating bending on 100Cr6 [**4**]. At a resistance level of UTS 1000 MPa, this lowering of fatigue limit between 10^7 and 10^{10} cycles is minimal, i.e. quasi negligible for martensitic and bainitic steels, higher for pearlitic steels, and much higher for ferrito-pearlitic steels. For cast aluminium and cast iron, the decrease of fatigue limit between 10^7 and 10^{10} cycles is always important (10 – 25 %).

A preliminary interpretation of the overall of these results can be proposed in terms of defects and homogeneity and/or the microstructure size. It is well known that when the defects exceed a critical size function of hardness, crack initiation occurs on these defects (inclusions, shrinkage, porosities ...), and not in the matrix. Thus, materials where the fatigue limit is govern by defect show their endurance limit decrease with the number of cycles, whereas materials where the endurance limit is govern by the matrix doesn't show evolution of the fatigue limit. This study provides guidelines to improve steel and also to have better component design by better knowledge of SN curve.

An interpretation of all of these results was also proposed in terms of defects and in-homogeneity and/or size of the microstructure. This hypothesis must however be validated.

5 CONCLUSIONS

To reach ecological goals fixed by European Union to carmakers, Engineers develop new technologies which are more and more demanding for steels. To face such requirement of steel with higher fatigue strength, steel makers should develop new solutions, based on better knowledge of the damage mechanisms of each component, the (steel grade + cleanliness + heat treatments or surface treatments) can be optimised, by using the support provided by simple and representative fatigue tests. Obviously, all these developments can only be achieved through a close collaboration with customers, who are the only one able to well know the in-service conditions of the different components.

Acknowledgements

The authors would like to thank CNAM ITMA, A2M Industrie, ARA, CNAM, ECM and RENAULT for fruitful collaboration in the different subjects presented in this paper.

6 REFERENCES

1 M. Langa, A. Ouakka, Mec. Ind., 2 (2001) 181-188.

2 Y. Murakami, "Metal fatigue: effects of small defects and non metallic inclusions", Elsevier (2002).

3 L. Engel, H. Klingele, "An atlas of metal damage", Wolfe Science Books, Vienna, (1981) p. 198.

4 Les aciers spéciaux – edited by Lavoisier (1997) - p. 533-554

5 H. Kitagawa, S. Takahashi, in Proc. 2nd Int. Conf. On “ behaviour of materials ” Boston – p. 627-631 (1976)

6 I. Chantier, V. Bobet, R. Billardon, F. Hild, Une approche probabiliste pour la prévision de la durée de vie en fatigue de structures en fonte GS, in 18èmes Journées de Printemps SF2M (Dimensionnement en fatigue de structures, démarches et outils).(1999)

7 J.L. Bernard - C.M. Sonsino, G.Baudry, Amorçage des fissures de fatigue sur les défauts de fabrication - Bilan des études menées dans le cadre européen BRITE, in Journées AFIAP – PARIS (Oct. 1989)

8 C.Bathias, N. Jingang, Determination of fatigue limit between 10^5 and 10^9 cycles using an ultrasonic fatigue device, in Advances in fatigue lifetime predictive techniques, ASTM STP , p. 141-152 (1993)

9 L. Manes, G. Baudry, C. Bathias, S. Rathery, J.F. Vittori, J.P. doucet, Gigacyclic fatigue in engineering steels, in Proc. Proc. of Int. Conf. Fatigue in the very high cycle regim Vienne (Vienna University (BOKU) edit.), p. 173 – 180, Juillet 2001

10 B. Champin, R. Tricot, R. Castro, “ contribution à l’étude de la résistance à la fissuration sous choc des aciers cémentés", ”revue de métallurgie , 1973

11 F. Da Costa, “ Comparaison de différents types de refroidissement après traitements thermochimiques et influence sur les caractéristiques mécaniques et métallurgiques. ”, ATTT Strasbourg, 2004